

MODELING THE CONTROL OF COVID-19: IMPACT OF POLICY INTERVENTIONS AND METEOROLOGICAL FACTORS

JIWEI JIA, JIAN DING, SIYU LIU, GUIDONG LIAO,
JINGZHI LI, BEN DUAN, GUOQING WANG, RAN ZHANG

ABSTRACT. In this article we propose a dynamical model with seven compartments to describe the transmission of COVID-19 in China. The home quarantine strategy has played a vital role in controlling the disease spread. Based on a Least-Squares procedure and officially published data, the estimation of parameters for the proposed model is obtained. The control reproduction number of most provinces in China are analyzed. Attention that the quarantine period must be long enough. Once the control strategy is removed, the disease still has high risk of human-to-human transmission continuously. In the study, a comprehensive meteorological index is introduced to represent the impact of meteorological factors. The effectiveness of vaccination is also considered in the model. We design detailed vaccination strategies for COVID-19 in different control phases and show the effectiveness of large scale vaccination.

1. INTRODUCTION

Coronavirus is a type of virus that causes infectious diseases in mammals and birds. Usually, the virus causes respiratory infections among people and the first infection was identified in the 1960s [30]. The main transmission routes of coronavirus are similar to other viruses: through sneezing, coughing, coming into contact with the infected people, or touching daily-used items [10]. On December 26, 2019, the first detected novel coronary pneumonia case in China was reported as an unknown etiology pneumonia in Wuhan, the capital of Hubei Province. Evidences pointing to the human-to-human transmission in hospitals and families were found in retrospective studies [33, 22, 4, 25]. It took a few days to arouse people's attention and the Chinese Center for Disease Control and Prevention (China CDC) isolated the first strain of the causative virus (SARS-CoV-2) successfully on January 7, 2020. With Chinese New Year migration, the large epidemics started in China and is spreading to many countries rapidly. On January 31, 2020, the World Health Organization (WHO) declared that the pneumonia outbreak caused by SARS-CoV-2 was a public health emergency of international concern [31]. Ten days later, WHO announced the official name of the disease caused by the novel coronavirus as COVID-19 [31] which is the seventh member of the family of coronaviruses that have infected humans [39]. As of February 19, 2020, there have been 74576 confirmed COVID-19

2010 *Mathematics Subject Classification.* 92D30, 37N25.

Key words and phrases. COVID-19; dynamical model; isolation strategy; vaccination strategy; meteorological index.

©2020 Texas State University.

Submitted February 22, 2020. Published March 16, 2020.

cases, causing 2118 deaths in China. Currently, there are over 100 countries around the world, which have reported over 30000 diagnosed cases.

Among the seven known human coronavirus, four of them are common pathogens of human influenza. The rest of them: SARS-CoV, MERS-CoV and SARS-CoV-2 are known to cause fatal respiratory diseases [30]. Although the coronavirus has been identified and analyzed for a long time, knowledge of the coronavirus is quite limited and there have been no known vaccines or antiviral drugs to prevent or treat human coronavirus infections. In 2003, a major coronavirus outbreak occurred in China was caused by SARS-CoV, resulting in an acute respiratory infectious disease with high fatality rate. The Chinese government and health organizations managed the outbreak of SARS through multiple control and prevention measures effectively. In contrast to SARS, the incubation period of COVID-19 is significantly longer. Different mean incubation periods of COVID-19 have been reported: 5.2 days [15] in an early study, 3.0 days [14] and 4.75 days [35] in a recent research. A patient with up to 24 days of incubation period is reported in [14] and a seemingly extreme case of 38 days was also reported in Enshi Tujia and Miao Autonomous Prefecture in Hubei Province. It is worthy noting that there seems to be a large number of people infected with asymptomatic [25] and the fatality rate is much lower than SARS-CoV and MERS-CoV [14]. Genetic studies of viruses show that the homology of SARS-CoV and SARS-CoV-2 is 85% [12]. However, SARS-CoV-2 binds ACE2 with higher affinity than SARS-CoV S [32]. By the end of January 29, 2020, the confirmed cases caused by COVID-19 had surpassed SARS. Overall, the uncertainty of the incubation period, a large number of asymptomatic cases and super transmissibility of the virus bring great difficulties in epidemic control.

Extensive research for COVID-19 with multiple perspectives has been reported. Corresponding diagnostic criteria and medication guide are designed and updated timely. Rapid detection reagent, anti-splash device for respirator and other special apparatus are brought into service quickly. The Chinese government started first-level response to major public health emergencies, the mechanism for joint prevention and control is established in a short period of time. As the disease evolves, COVID-19 is no longer just a medical problem, it has also become a far reaching socioeconomic concern. For this reason alone, collecting massive data relating to COVID-19 and analyzing the inherent linkage among these data are of great importance for the next step of control strategy. To this end, epidemic dynamics and population ecology are among the key methods. Mathematical model is an important tool to study infectious diseases, such as measles [21], fever [19], TB [16], hepatitis [38] and other normal epidemics. It is also an excellent tool in the investigation of actual outbreaks, like mosquito-borne [23, 28], MERS [34], SARS [37] and Ebola [26].

Dynamical modeling of COVID-19 transmission has been performed by many scholars. A modified SEIR model with eight components is proposed by Tang *et al.* [27], where the control reproduction number under their estimation is 6.47. The travel related risks of disease spreading were evaluated in [3], which predicted the potential of domestic and global outbreak. The effect of travel restriction in Beijing was also discussed in [33]. It shows that with the travel restriction (no imported exposed individuals to Beijing), the number of infected individuals in seven days can decrease by 91.14%, compared with the scenario of no travel restriction. A Bats-Hosts-Reservoir-People network was developed in [5] for simulating the potential

transmission from the infection source (likely bats) to the human infection and the analytic form of basic reproduction number for a simplified Reservoir-People network was calculated. Ming *et al.*[17] applied a modified SIR model to project the actual number of infected cases and the specific burdens on isolation wards and intensive care units (ICU). The estimation suggests that assuming 50% diagnosis rate with no public health interventions implemented, the actual number of infected cases could be much higher than reported. Chen *et al.* [6] proposed a novel dynamical system with time delay to present the incubation period behavior of COVID-19, where the estimated parameters show that the prediction is highly dependent on the population size and public policies executed by local governments.

In this article, we propose an extended SEIR model to describe the transmission of COVID-19 in China. In order to prevent the epidemic from worsening, the Chinese government has pursued the strictest isolation strategy for all people throughout the country to restrict the population mobility. Traffic control, limitation of travel, extension of the Chinese New Year vacations, delay of returning to work, rigorous management of communities and even the wartime management have ensured that the susceptible population stay home. At this stage, the main aim of the disease control is ‘preventing the disease spreading inside’. The proposed model in this study mainly focuses on the home quarantine strategy. The strategy requires people to stay at home for at least 14 days, aiming at reducing the chance of contact with the infected people as much as possible. The asymptomatic transmission and isolation treatment policy are also taken into account in this paper. The official data published by China CDC and a Least-Squares procedure are employed to estimate the parameters. The cases of most provinces in China are simulated and the control reproduction number (\mathcal{R}_c^0) are calculated for each selected provinces. To capture the variation of effective control reproduction number ($\mathcal{R}_c(t)$), the control process are divided into three periods, the average of $\mathcal{R}_c(t)$ are calculated for each stage and the results inside and outside Hubei province are compared. The numerical results show that the intervention and support strategy carried out by the government decreases the effective control reproduction number quickly. Besides the unprecedented home quarantine policy, the Chinese government also provides free medical care for the diagnostic COVID-19 patient. Furthermore, as of 24:00 on February 14, 217 medical teams (military medical teams are not included) including 25633 team members have arrived Hubei from all over China. It greatly relieved the medical pressures of Hubei Province. In our analysis, we estimate the disease burden by means of accumulated medical resource needed in 90 days, the peak value and peak time of the diagnostic population are also given in the numerical simulation part.

Study shows that SARS-CoV and SARS-CoV-2 share high homology with genes [12]. Therefore, there should be similarity between them. Back in 2003, there was no vaccine or specific medicine for SARS. However, it seemed to disappear quickly at the start of May. Weather was considered as an important factor for the vanishing of SARS [7, 8]. It has been pointed out that high temperature can weaken the activity of SARS-CoV [18]. Spring will soon come in China and the meteorological measures, such as temperature and humidity, will change quickly. To study the relationship between the meteorological conditions and the transmission of COVID-19, we obtain the weather data from China Meteorological Data Service Center (CMDC) and define a comprehensive meteorological index MeI . The outbreak of

COVID-19 coincides with Chinese New Year Migration, we define an index MiI to describe the migration level, based on the value of MiI , we separate all the selected provinces into two groups, the high and low level groups. The correlation analysis shows that the spread rate are significantly associated with MeI in each group. The air index plays an important and interesting role, it is a positive factor in the low-migration group, but negative in the high-migration group. On the other hand, our study shows that the high relative humidity helps control the spread of COVID-19 for both groups.

The third major factor considered in our model is vaccination strategy as some progresses on the vaccines for COVID-19 have been reported. For this purpose, we replace the quarantined compartment with the vaccinated in the proposed model to study the effect of vaccination. We simulate three scenarios to represent the vaccination starting from the three control phases: the first 7 days (prophase), the next 7 days (metaphase) and the following 14 days (anaphase). The results show that the efficient vaccination accelerates the diagnostic population to the peak and contributes to reducing the effective control reproduction number effectively.

The rest of the paper is organized as follows. Based on the proposed dynamical model, we analyze the current control strategy in Section 2. We discuss the impact of meteorological factors and vaccines in Section 3. Finally, we present some concluding remarks in Section 4.

2. ANALYSIS FOR CURRENT CONTROL STRATEGY

2.1. Model formulation. Based on the epidemiological feature of COVID-19 and the isolation strategy being carried out by the government, we extend the classical SEIR model to describe the transmission of COVID-19 in China. In particular, we use a short-term model to describe the strictest isolation strategy, the total population is relatively fixed. Consideration must be given to both the actual situations and theoretical analysis, some simplifications are necessary. This model satisfies the following assumptions.

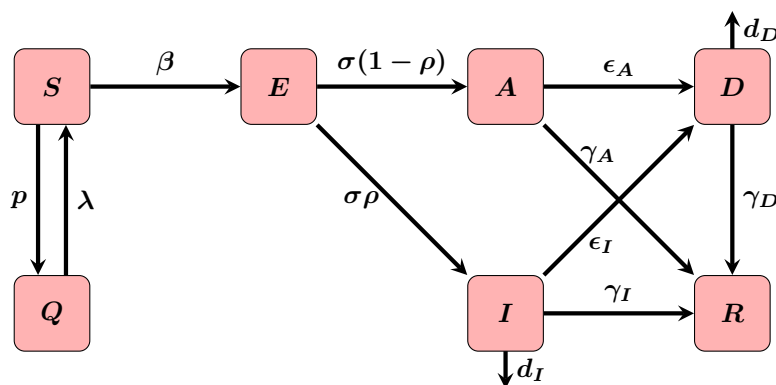


FIGURE 1. Flow diagram of the compartmental model of COVID-19 in China

- (1) All coefficients involved in the model are positive constants.
- (2) Natural birth and death rate are not factors.

- (3) Once the infected patient is cured, the immune efficacy will maintain for some time, i.e., second infection is not considered in the model.

Based on the above assumptions and the actual isolation strategy, the spread of COVID-19 in the populations is depicted in Figure 1.

Using the above depiction, we formulate the corresponding dynamical model as follows.

$$\begin{aligned}
 \frac{dS}{dt} &= -\beta S(I + \theta A) - pS + \lambda Q \\
 \frac{dQ}{dt} &= pS - \lambda Q \\
 \frac{dE}{dt} &= \beta S(I + \theta A) - \sigma E \\
 \frac{dA}{dt} &= \sigma(1 - \rho)E - \epsilon_A A - \gamma_A A, \\
 \frac{dI}{dt} &= \sigma\rho E - \gamma_I I - d_I I - \epsilon_I I \\
 \frac{dD}{dt} &= \epsilon_A A + \epsilon_I I - d_D D - \gamma_D D \\
 \frac{dR}{dt} &= \gamma_A A + \gamma_I I + \gamma_D D
 \end{aligned} \tag{2.1}$$

where $S(t)$, $E(t)$, $I(t)$, $R(t)$, $Q(t)$, $A(t)$ and $D(t)$ denote the individuals who are susceptible, exposed, infectious with symptoms, recovered, home quarantined, asymptotically infected and diagnosed at time t , respectively. It should be made clear that the exposed individuals $E(t)$ represent low-level virus carriers, which are considered to be no infectiousness. For the home quarantined individuals $Q(t)$, we assume, due to severe travel restrictions and rigorous supervision by their local communities, that they have no contact with infected individuals. As far as the diagnosed individual $D(t)$ are concerned, we assume that they are being treated and isolated.

There are a total of 12 model parameters in system (2.1). The main task of this paper is to approximate these parameters with the publicly available official data. We adopt bilinear incidence rates to describe the infection of the disease and use parameter β to denote the contact rate. It is reasonable to assume that the infection rate of the individuals with no symptoms is lower than rate of those with symptoms. In (2.1) we use $\theta \in (0, 1)$ to denote the ratio between the two rates. Concerning the home quarantined population, we use parameters p and λ to represent the quarantined rate and release rate of quarantined compartment, respectively. Transition rate of exposed to infected class is denoted as σ . Once infected, the proportion of becoming symptomatic is denoted by ρ , which means that the proportion of asymptomatic is $1 - \rho$. Diagnostic rate of asymptomatic and symptomatic infectious are respectively denoted by ϵ_A and ϵ_I and the mean recovery period of class A, I, D are denoted by $1/\gamma_A, 1/\gamma_I$ and $1/\gamma_D$, respectively. The parameters d_I and d_D represent the disease-induced death rate.

Under the isolation control strategy, we employ the next generation matrix approach [13] to calculate the control reproduction number,

$$\mathcal{R}_c^0 = r(\mathcal{F} \cdot \mathcal{V}^{-1}) = \left(\frac{\beta\theta(1-\rho)}{\epsilon_A + \gamma_A} + \frac{\beta\rho}{\gamma_I + d_I + \epsilon_I} \right) S_0. \tag{2.2}$$

where r denotes the spectral radius and

$$\mathcal{F} = \begin{pmatrix} 0 & \beta S \theta & \beta S \\ 0 & 0 & 0 \\ 0 & 0 & 0 \end{pmatrix}, \quad \mathcal{V} = \begin{pmatrix} \sigma & 0 & 0 \\ -\sigma(1-\rho) & \epsilon_A + \gamma_A & 0 \\ -\sigma\rho & 0 & \gamma_I + d_I + \epsilon_I \end{pmatrix},$$

and define the corresponding effective control reproduction number is

$$\mathcal{R}_c(t) = \left(\frac{\beta\theta(1-\rho)}{\epsilon_A + \gamma_A} + \frac{\beta\rho}{\gamma_I + d_I + \epsilon_I} \right) S(t). \quad (2.3)$$

As we see in the following sections, $R_c(t)$ provides us a clear index to evaluate the control strategy at any time t .

2.2. Data-driven parameter estimation.

Data preparation. On January 23, 2020, China CDC and all provincial CDCs started to publish the epidemic data in their official websites. In this study, we collect these data up to February 19 for the purpose of parameter estimation. There are 28 days in the data collection period, which are twice as many as the least home quarantine period. According to the average incubation period, we divide the total control period into three phases: prophase (1-7 days), metaphase (8-14 days) and anaphase (15-28 days). We note that crucial variable $D(t)$ in model (2.1) can be calculated from the published data by subtracting the recovered and death cases from the accumulated diagnosed cases. The counting rule of $D(t)$ is subtraction, which avoids the loss of data immensely. We take $D(t)$ as the benchmark in our data fitting simulation. We also note that since Qinghai and Tibet have only few of diagnostic cases and the epidemic is already under control by the government, these two provinces are excluded in our research. In addition, Hong Kong, Macao and Taiwan are also excluded because of their different diagnostic criteria and control strategy.

Parameter estimation and prediction procedure. In order to estimate \mathcal{R}_c^0 and $\mathcal{R}_c(t)$, we use the daily published data to perform fitting. The data pre-processing is as above mentioned, the base time unit is one day. Based on the publicly known facts, we have the following assumptions and estimations on the parameters. According to the response of each province, $1/p$ is estimated as 3 to 5 days, $1/\lambda$ is taken as 60 days for most provinces. The mean incubation period ($1/\sigma$) is about 7 days [24, 27]. Based on the percentage of symptomatic infected patients reported in [24], we estimate that the proportion of symptomatic in the infected class is in [0.7, 0.99]. Although the testing kits are developed and brought into service quickly, the shortage delayed the diagnosis. Based on the detailed data of confirmed cases, the average time of diagnosis ($1/\epsilon_I$) for infectious with symptoms is taken to be in the interval [3, 9]. The diagnosis of a symptomatically infected is much harder, we estimate the period ($1/\epsilon_A$) as 3 to 15 days. Luckily, the spread ability of asymptomatic infected is limited and based on the data we have collected, we set the parameter $\theta \in [0.005, 0.2]$. Using parameters d_D and γ_D in model (2.1), the mortality rate (mr) of disease can be written as

$$mr = \frac{d_D}{d_D + \gamma_D}.$$

Based on the collected data, we set mr as 2.1% for most provinces. The death rate of patients without effective medical care will be higher, we describe it as

$d_I = c_I \cdot d_D$, where $c_I \in [1.1, 1.6]$. The relationship in average recover period is assumed to be $\gamma_A = c_A \cdot \gamma_I$ and $\gamma_D = c_D \cdot \gamma_I$, where $c_A, c_D \in [1.1, 1.5]$. The reason is that the speed of recovery in asymptotically infected and patients with proper medical care is faster than those infected without treatment.

We employ a Least-Squares procedure to estimate parameters β and γ_I . Assuming that we have a proper estimations for other parameters in (2.1), we need to solve the following optimization problem.

$$\min_{\beta, \gamma_I} \|D(t; \beta, \gamma_I) - D_{pub}\|_2, \quad (2.4)$$

where D_{pub} is the number of diagnosed individuals in medical treatment obtained from the data published by CDC. Then the estimation and prediction procedure are as follows.

- (1) Set the initial condition $\{S(t_0), Q(t_0), E(t_0), A(t_0), I(t_0), R(t_0)\}$ and the proper guesses for the parameters in (2.1) other than β and γ_I .
- (2) Based on the officially published data D_{pub} , solve the optimization problem (2.4) to obtain the estimations β^* and γ_I^* for β and γ_I , respectively.
- (3) Based on β^* and γ_I^* , the initial condition and parameters set in Step (1), solve the dynamical system (2.1) to obtain $S(t), Q(t), E(t), A(t), I(t), R(t)$ and $D(t)$.

Remark 2.1. For initial values, the total population is based on the report published by the National Bureau of Statistics [20]. Because of the Chinese New Year, many were on vacation and stayed at home when the outbreak started. We estimate the fraction of original home quarantine as about 30%.

Remark 2.2. Because of the change of diagnostic criteria from nucleic acid detection to clinical diagnosis, there was a big jump for D_{pub} of Hubei Province on February 12, 2020 (see Figure 2(b)).

Accumulated medical resource estimation. To avoid the delay of medical treatment caused by personal economic incapability, the Chinese government started to carry out free medical care strategy at the very early stage of the epidemic. Nationally financed support provided timely treatment for COVID-19 patients. To measure the effectiveness of the financial support for the disease treatment, we introduce an index called accumulated medical resource (*AMR*) up to time t_f defined by

$$AMR = k \int_0^{t_f} D(t) dt, \quad (2.5)$$

where the parameter k represents the average index of medical resource a patient needs daily.

2.3. Numerical simulation. The first confirmed COVID-19 patient of China was located in Wuhan, the capital of Hubei Province. Because of limited knowledge of the disease, the control measure in Wuhan was inadequate at the beginning, which resulted in the outbreak of COVID-19 in Hubei Province. Because of the different circumstances inside and outside Hubei Province, the estimation and prediction are investigated separately. Notice that, the spread of COVID-19 is very fast. In [36], the leading Chinese epidemiologist Nanshan Zhong and his co-authors declare that the disease may be controlled well by the end of April under China's powerful control strategy. Based on this, we take the parameter $1/\lambda$ as 90 days. Following the procedure in Section 2.2, the estimated parameters β and γ_I are obtained, and

the results of inside and outside Hubei province are presented in Figure 2, where the blue solid line shows the fit of diagnosed population $D(t)$ based on current circumstances. Asterisks represent D_{pub} . The trends until the end of April are also shown in Figure 2. In Table 1, we list all the other parameters, initial values and the corresponding \mathcal{R}_c^0 inside and outside of Hubei Province. We find that the \mathcal{R}_c^0 outside Hubei is much higher than that in inside Hubei. This is mainly caused by the huge size of Chinese population. To evaluate the unprecedented strict isolation strategy, we calculate the average $\mathcal{R}_c(t)$ for three stages and the result are shown in Table 2. We can clearly see that the values of the average $\mathcal{R}_c(t)$ decrease quickly under current control strategy. It almost went down to 1 in metaphase outside Hubei Province and now is below 1. The situation in Hubei Province is more complex, though the average $\mathcal{R}_c(t)$ decreases sharply, it is still greater than 1 in anaphase. We emphasize that the disease is still not under control completely and has a high risk of sustainable spread. The strictest isolation strategy has made great contribution to the prevention of the disease spread and needs to continue in the absence of effective medicine and vaccine.

TABLE 1. Parameters and initial values inside and outside Hubei

Parameter	Outside	Inside	Parameter	Outside	Inside
β	5.5010×10^{-9}	1.0014×10^{-7}	ϵ_I	1/4	1/3
θ	0.1000	0.1600	γ_A	0.1496	0.1500
p	1/3	1/6.2	γ_I	0.0998	0.1000
λ	1/90	1/90	γ_D	0.1496	0.1400
σ	1/7	1/7	d_I	0.0046	0.0105
ρ	0.8800	0.8800	d_D	0.0031	0.0030
ϵ_A	1/5	1/10			
\mathcal{R}_c^0	12.7700	8.5423			
$S(0)$	921984900	41419000	$I(0)$	563	1206
$Q(0)$	414225100	17751000	$D(0)$	227	494
$E(0)$	3207	2280	$R(0)$	3	31
$A(0)$	595	1450			

TABLE 2. Average $\mathcal{R}_c(t)$

	Prophase	Metaphase	Anaphase
Outside Hubei	6.0295	1.0843	0.6208
Inside Hubei	5.6870	2.2426	1.0560

To make a better illustration of quarantine strategy, we test different home quarantine periods ($1/\lambda$) in Figure 2. The corresponding peak value and peak time (T_{peak}) of $D(t)$ and the accumulated medical resource needed in 90 days defined

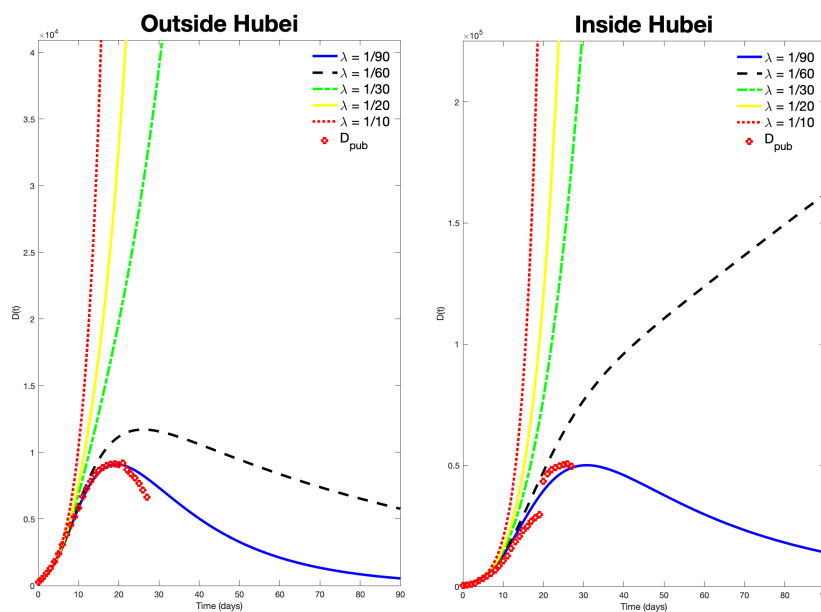


FIGURE 2. Optimal simulation and prediction of the transmission trend

in (2.5) are listed in Table 3. In Figure 2, the colored dashed lines show that if the quarantine period is not long enough, the isolation strategy does not work well. There needs a longer quarantine period in Hubei Province than outside. Figure 2 also indicates that the longer quarantine period, the earlier peak time of $D(t)$ arrives.

The ward for COVID 19 is unlike most of the infectious diseases. To avoid nosocomial infection, it requires maximal barrier precautions in the hospital and there are quite a few critically ill patients in ICU. The Chinese medical system is facing the huge challenges due to rapidly increasing number of patients, especially at the peak value of $D(t)$. The study of the maximum capacity to deal with the emergency is necessary for disease control. In the simulation, the peak time of $D(t)$ is February 12 outside of Hubei and February 24 inside Hubei, which is in line with the actual data (the last line in Table 3). By adjusting the parameter λ , we find that, if the quarantine period is fixed as 30 days, both the peak value and AMR are more than tripled as now inside Hubei. Particularly, the peak time would not be reached in three months in Hubei. The situation outside Hubei is not much better than that inside Hubei. The peak time delays by a week. Though the peak value does not increase by much, the AMR almost doubles. More details of shorter quarantine periods are shown in Table 3. Notice that, in shorter quarantine periods (5, 10 and 20 days), T_{peak} seems proportional to $1/\lambda$. It is mainly caused by a large amount of infected population. As a consequence, the medical burden in shorter quarantine periods situation are extremely heavy.

So far our study has provided an intuitionistic understanding of COVID-19 in China. In what follows, we study the transmission and control strategy of COVID-19 province by province according to the unique characteristic of each one of them. The province-wise simulation results are shown in Figure 3 with blue solid lines.

TABLE 3. Peak value, peak time of $D(t)$ and AMR during 90 days.

	Outside Hubei			Inside Hubei		
$1/\lambda$	$Peak$	T_{peak}	AMR	$Peak$	T_{peak}	AMR
90	9094	20	354017k	50041	32	2649863k
30	11706	27	743494k	161780	*	8342449k
20	1540394	*	25210395k	2503084	78	100643586k
10	47382685	*	618221390k	4372193	60	185123007k
5	142619535	67	4664793399k	7810630	45	264760516k
Data	9211	22	-	50633	27	-

¹ * do not reach peak in 90 days.

² - not applicable.

The colored dashed lines represent the trends of $D(t)$ under different quarantine periods. All the parameters are shown in Appendix Table 8 and Table 9. The peak value and peak time of $D(t)$ for each province under different λ are given in Appendix Table 7. Our model fits the published data accurately for most of the provinces. \mathcal{R}_c^0 are estimated for each province and displayed in Figure 4. The simulation results show that, without the effective control strategy, the disease would have been out of control in every province. On the other hand, the results in Figure 3 show the proper duration of the quarantine periods for each province. The home quarantine periods in most provinces can be much shorter than Hubei and the disease can also be under control. We also find that, the trends of $D(t)$ between 30 days and 60 days quarantine periods are similar for GanSu, Tianjin, Yunnan and so on, it suggests that the general public of these provinces can return to work under orderly organization. However, Inner Mongolia, Xinjiang and Heilongjiang need to be more cautious, they are in the key period of the disease control.

The medical resources in each province are distributed unevenly. After the disease outbreak, the Chinese government deployed medical resources to rescue Hubei Province. We estimate the AMR needed for each provinces by integrating $D(t)$ from 0 (Jan 23) to 90 (Apr 22) days under different quarantine periods (5 – 60 days). The detail parameter values and corresponding AMR in 90 days are shown in Table 7. We collect the number of 3A hospital (the hospitals with the highest comprehensive index, such as medical level, capacity etc.) in each province, which can reflect the level of medical resources. In Table 4, we show the 3A hospital (N_3) number in each province, where the medical burden (MB) is measured by

$$MB_3 = \frac{AMR}{N_3}.$$

The value of AMR is taken as the optimal simulation results, i.e., $\lambda = 1/60$. The median of MB_3 among 29 provinces is 461k, Thus more attention should be paid to those provinces whose MB_3 indices are over the median value. Since disease outbreak, the government established many designated hospitals and fever clinics to relieve the stress of medical resources. Denote by N_d the number of designated

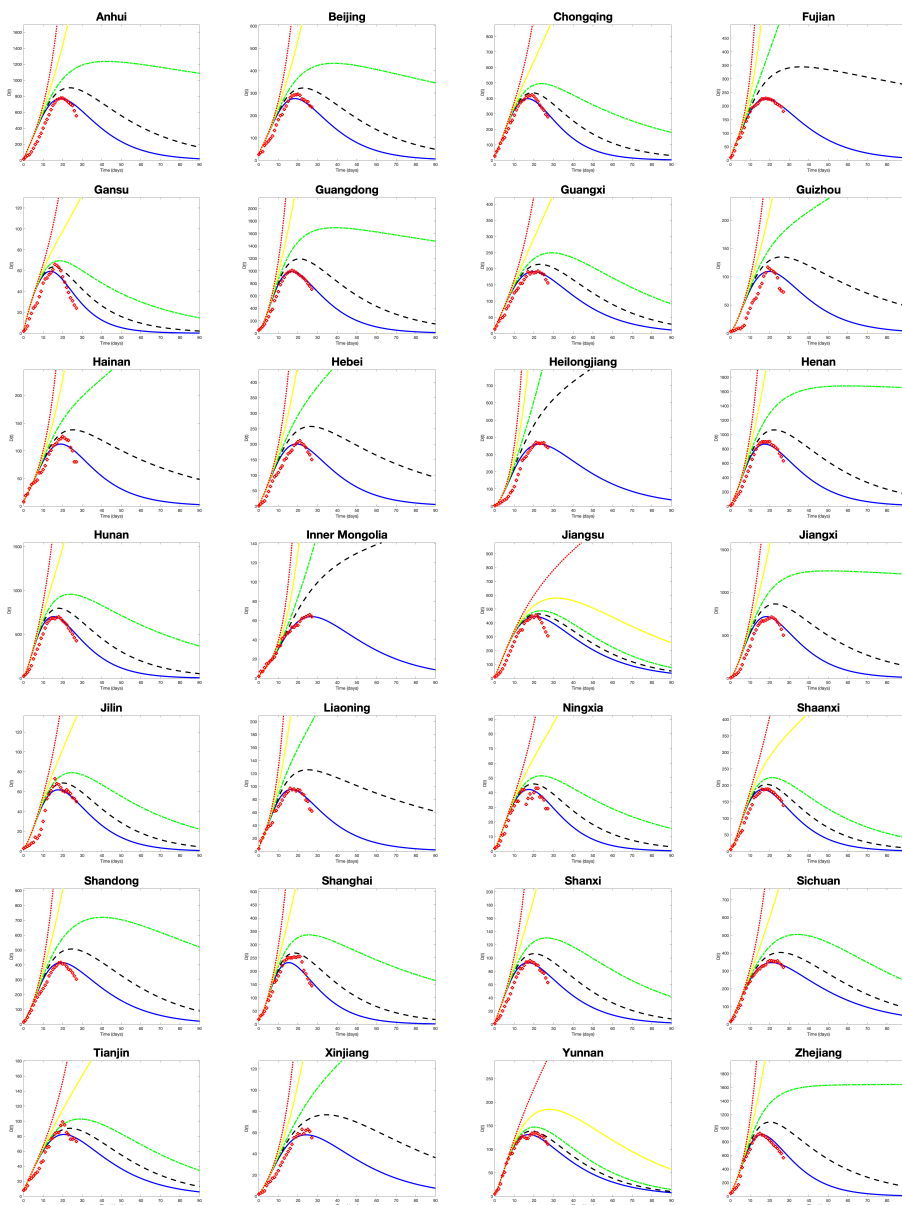


FIGURE 3. Simulation results of $D(t)$ (Solid blue line: $\lambda = 1/60$, dashed dark line: $\lambda = 1/30$, dash-dot green line: $\lambda = 1/20$, solid yellow line: $\lambda = 1/10$, dotted red line: $\lambda = 1/5$) and published data D_{pub} (Red asterisk).

hospital, we set a weight between the 3A hospital and designated hospital. The weighted medical burden is described as

$$MB_W = \frac{AMR}{3 * N_3 + (N_d - N_3)}.$$

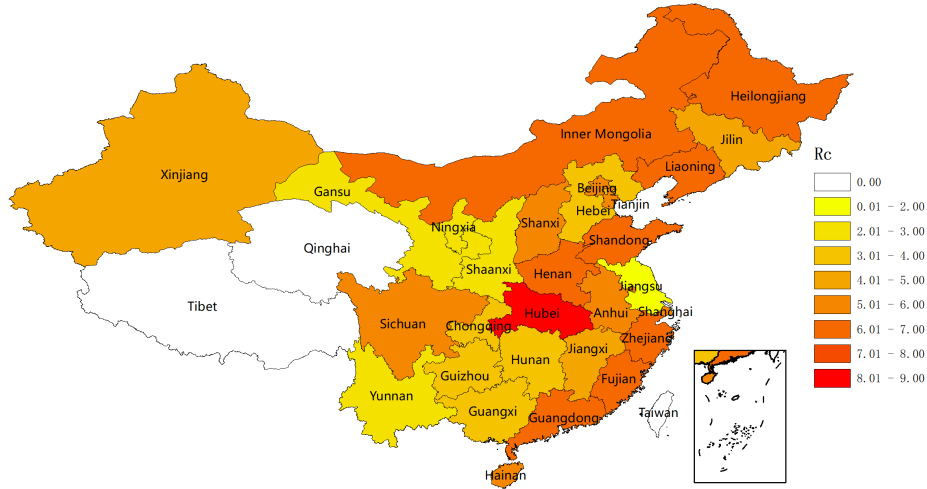


FIGURE 4. \mathcal{R}_c^0 distribution heat map

TABLE 4. AMR , $3A$ and designated hospital comparison

Province	Anhui	Beijing	Chongqing	Fujian	Gansu	Guangdong	Guangxi	Guizhou
AMR	28759k	10216k	12705k	8866k	1639k	32278k	8093k	4203k
N_3	20	30	11	24	12	66	25	23
N_d	271	90	104	765	99	886	48	1143
MB_3	1438k	341k	1155k	369k	137k	489k	324k	183k
MB_W	92k	68k	101k	11k	13k	32k	83k	4k
Province	Hainan	Hebei	Heilongjiang	Henan	Hubei	Hunan	Inner Mongolia	Jiangsu
AMR	4078k	7495k	16502k	30486k	2649863k	21867k	3167k	20035k
N_3	5	32	31	24	36	20	13	38
N_d	317	394	493	508	678	325	213	769
MB_3	816k	234k	532k	1270k	73607k	1093k	244k	527k
MB_W	12k	16k	30k	55k	3533k	60k	13k	24k
Province	Jiangxi	Jilin	Liaoning	Ningxia	Shaanxi	Shandong	Shanghai	Shanxi
AMR	24493k	2086k	3336k	1384k	6093k	16992k	7036k	3371k
N_3	33	20	36	3	25	21	24	32
N_d	307	133	228	73	354	541	29	205
MB_3	742k	104k	93k	461k	244k	809k	293k	105k
MB_W	66k	12k	11k	18k	15k	29k	91k	13k
Province	Sichuan	Tianjin	Xinjiang	Yunnan	Zhejiang			
AMR	16921k	3660k	2868k	5330k	28601k			
N_3	36	17	9	5	26			
N_d	1910	27	176	350	323			
MB_3	470k	215k	319k	1066k	1100k			
MB_W	9k	60k	15k	15k	76k			

Comparing the value of MB_3 with MB_W in each province, we can clearly see that, the addition of designated hospitals has decreased the medical burden sharply and resulted in earlier diagnosis, earlier isolation and better treatment. But the

disease burden in Hubei is still huge, it is almost 60 times greater than other province. On one hand, we have taken full advantage of current medical resources; on the other hand, the additional medical workers and materials from other province are supported to Hubei Province spare no effort. Sufficient and effective medical support is the basic foundation to control COVID-19.

3. FURTHER TRENDS FOR THE CONTROL OF COVID-19

In previous section, the transmission of COVID-19 inside and outside Hubei was discussed. Simulations for most provinces can conduce to understand the effect of control strategy in China. And the corresponding analysis for medical resources are given. Isolation strategy plays an important role in the prevention of disease spreading. But the strictest isolation strategy brings great inconvenient to people's daily life. Now the disease spread is in decline, more and more people will return to their normal life. In this section, we explore future control strategy from the meteorological and vaccine perspective for the following control phase.

3.1. The impact of meteorological index (MeI). Seventeen years ago, SARS outbreaked in China and it spread quickly and disappeared suddenly. There was no specific medicine and vaccine, the medical level and control strategy were not as complete as today. Meteorological factor is regarded as a critical role for the vanishing of SARS [7, 8]. Due to the high genetic homology of SARS-CoV and SARS-CoV-2, it is logical to exam the meteorological impact on the spreading of COVID-19. To this end, we collect the official published average meteorological data during the simulation period, including air index (AI), temperature (TE), precipitation (PR), relative humidity (RH) and wind power (WP) from China Meteorological Data Service Center (CMDC) website [9] for correlation analysis.

The outbreak of COVID-19 coincided with the Chinese New Year and the population migration was the busiest of the year. Wuhan is the China's major transportation hub connecting nine provinces in central and south central China with a large number of people moving out or passing by the city. Needless to say, population migration is a key factor in the spread process. To study this factor, we define the following index MiI for each provinces to reflect the population migrate from Hubei Province,

$$MiI = C \frac{PE}{DIS^2},$$

where PE is the percentage of population moving in from Hubei, DIS is the distance between the capital of destination province and Wuhan and $C = 10^{10}$ is an adjustment constant. The parameter PE and DIS are obtained from Baidu Migration [2] and Baidu Map [1].

Based on the descending order of MiI for provinces other than Hubei (see Table 5 for details), we classify them as Group I and Group II to represent different migration levels. With the critical value set as $MiI_y = 100$, the MiI is greater than MiI_y in Group I and less than MiI in Group II. From Table 5, one can see that most of the high MiI provinces are those surrounding Hubei Province.

Based on above grouping criteria, we use the following formula and linear regression procedure to calculate a comprehensive meteorological index MeI and apply the correlation analysis to \mathcal{R}_c^0, β and MeI for each group as follows.

$$MeI = c_1 \ln(AI) + c_2 TE + c_3 PR^2 + c_4 RH + c_5 WP + c_6. \quad (3.1)$$

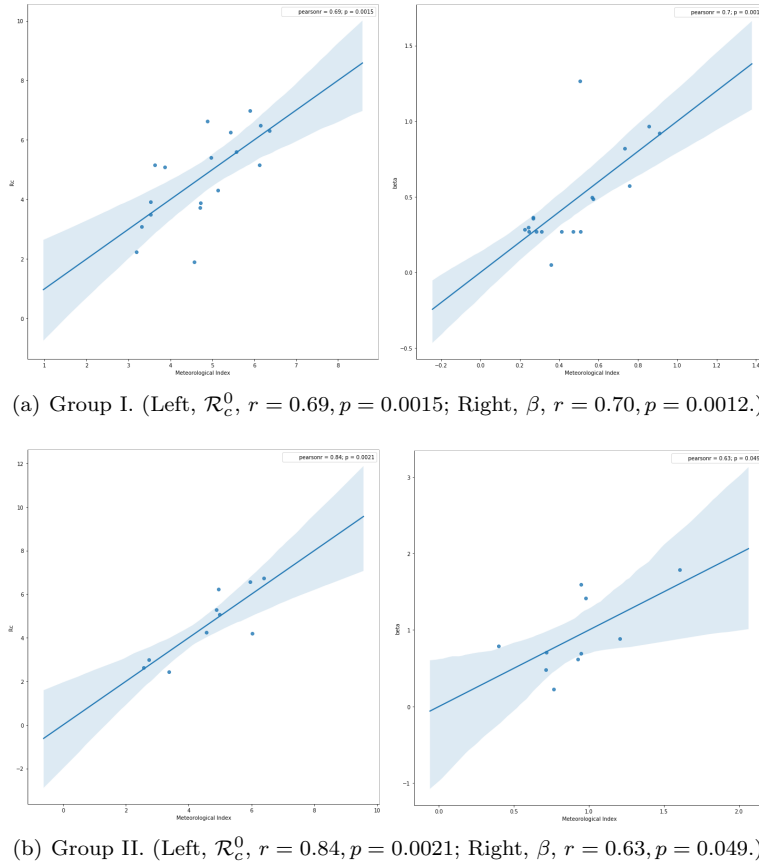


FIGURE 5. Correlation analysis of \mathcal{R}_c^0 , β and MeI .

The coefficients and intercepts are listed in Table 6. For each group, we calculate $MeI_{\mathcal{R}_c^0}$ and MeI_{β} and perform the correlation analysis with \mathcal{R}_c^0 and β , respectively. The results are presented in Figure 5. It shows that \mathcal{R}_c^0 and β are significantly correlated with MeI .

The coefficients in Table 6 indicate that the impact of meteorology factors on the disease spread is quite different between the two groups. For example, air index is the most important meteorology factor in our study. In high MeI group, $\ln(AI)$ is inversely proportional to $MeI_{\mathcal{R}_c^0}$. However, in low MeI group, the result is reversed. The reason is that, the fraction of imported cases is high in high MeI group. If the value of AI is small, it represents good air condition. As a result, the social activities will increase and the probability of contact with infected people will also increase. In low MeI group, the bad air condition will aggravate the spread. The impact of wind power in both group has a similar pattern. Bad air condition and strong wind suggest that people should pay more attention to personal protection. In high MeI group, higher temperature will cause undesirable impact on the control of disease. However, in low MeI group, the result shows that higher temperature will reduce the spread. Precipitation shows low influence on COVID-19 spread.

TABLE 5. Migration Index Computation

Province	Hunan	Jiangxi	Henan	Anhui	Jiangsu	Chongqing	Guangdong
<i>PE</i>	15.65%	7.75%	18.66%	6.58%	3.86%	8.23%	7.27%
<i>DIS</i>	284.4	254.5	468.2	304.3	452.3	759.1	835.9
<i>MiI</i>	19349	11965	8512	7106	1887	1428	1041
Province	Zhejiang	Shaanxi	Shandong	Fujian	Sichuan	Hebei	Shanghai
<i>PE</i>	3.1%	3.59%	2.74%	2.47%	4.49%	1.84%	1.13%
<i>DIS</i>	558.3	662.5	726.1	690.3	985.4	836.6	684.7
<i>MiI</i>	995	818	520	518	462	320	241
Province	Guizhou	Shanxi	Guangxi	Beijing	Yunnan	Gansu	Hainan
<i>PE</i>	1.68%	1.25%	1.98%	1.44%	1.24%	0.84%	0.86%
<i>DIS</i>	869.5	825.8	1048.1	1054.7	1295.3	1155	1242.1
<i>MiI</i>	222	183	180	130	74	63	56
Province	Liaoning	Tianjin	InnerMongolia	Heilongjiang	Jilin	Ningxia	Xinjiang
<i>PE</i>	0.67%	0.28%	0.32%	0.52%	0.36%	0.11%	0.26%
<i>DIS</i>	1480.4	976.6	1161.4	2000.2	1760.4	1145.6	2770.4
<i>MiI</i>	31	29	24	13	12	8	3

TABLE 6. Linear regression coefficients and intercept for \mathcal{R}_c^0, β and MeI .

	c_1	c_2	c_3	c_4	c_5	c_6
Group I						
$MeI_{\mathcal{R}_c^0}$	-2.0598	0.1193	1.6884×10^{-4}	-0.1439	0.1843	21.5757
$MeI_{\beta}(\times 10^{-8})$	-6.6671	-0.2991	3.9571×10^{-4}	-0.1833	-2.1504	50.3030
Group II						
$MeI_{\mathcal{R}_c^0}$	1.8802	-0.1799	0.0132	-0.1390	1.1656	-0.3215
$MeI_{\beta}(\times 10^{-8})$	2.5854	0.0188	0.0269	-0.1984	-2.1882	9.7468

Notice that, the results in both groups show that higher relative humidity is the protection factor for the disease control.

3.2. Further control with new vaccine. On February 22, 2020, Zhejiang Provincial Government reported some progress on the vaccine of SARS-CoV-2. It is claimed that the first vaccine has produced antibodies and the process is in the animal experiment stage [11]. The Director-General of WHO said that more than 20 COVID-19 vaccine candidates are currently in development phase and some new treatments are in clinical trials, the results are expected within a few weeks [29]. The progress of the development of vaccines is much quicker than expected. If the new vaccine of COVID-19 is brought into service, it will greatly benefit the the control of the disease. In regards to the strictest isolation strategy, from the mathematical point of view, the strategy is just like a short-time vaccine for the susceptible population. The effect of staying away from the source of infection is the same as contacting with infected people but being immune from being infected.

After a slight modification on model (2.1), we can describe the impact of the vaccine, by replacing the quarantine compartment Q with the vaccine compartment V and setting parameter p as the vaccination rate, $1/\lambda$ as the mean protection period of the new vaccine.

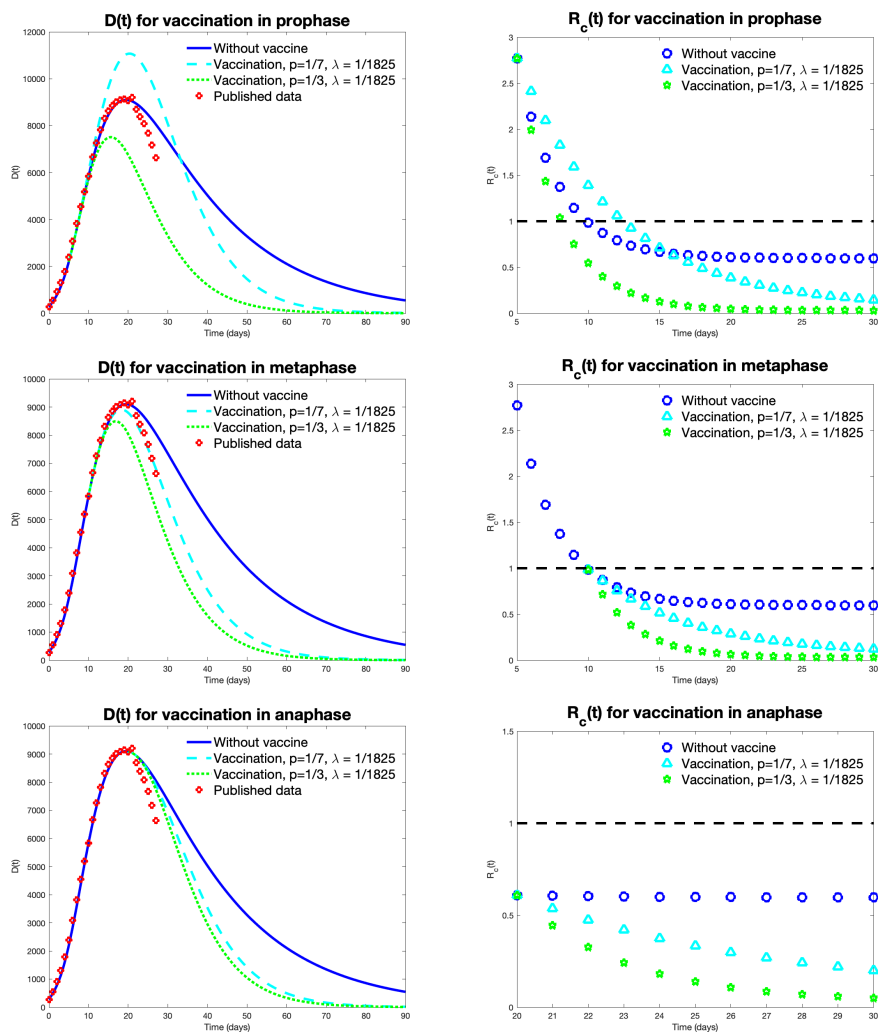


FIGURE 6. Impact of vaccination strategy outside Hubei Province

Though no vaccine has been brought into service, the theoretical analysis can be useful to make better control. In this section, we show the effect of different starting time of vaccine usage inside and outside Hubei Province. Considering the three control phases defined earlier, we take the starting day on January 28 (prophase), February 2 (metaphase) and February 12 (anaphase). We assume the average vaccination period is five year, which means $\lambda = 1/1825$. We test different values of parameter p to present the impact of vaccination efficiency. The corresponding numerical results are shown in Figure 6 and Figure 7. In the area outside Hubei

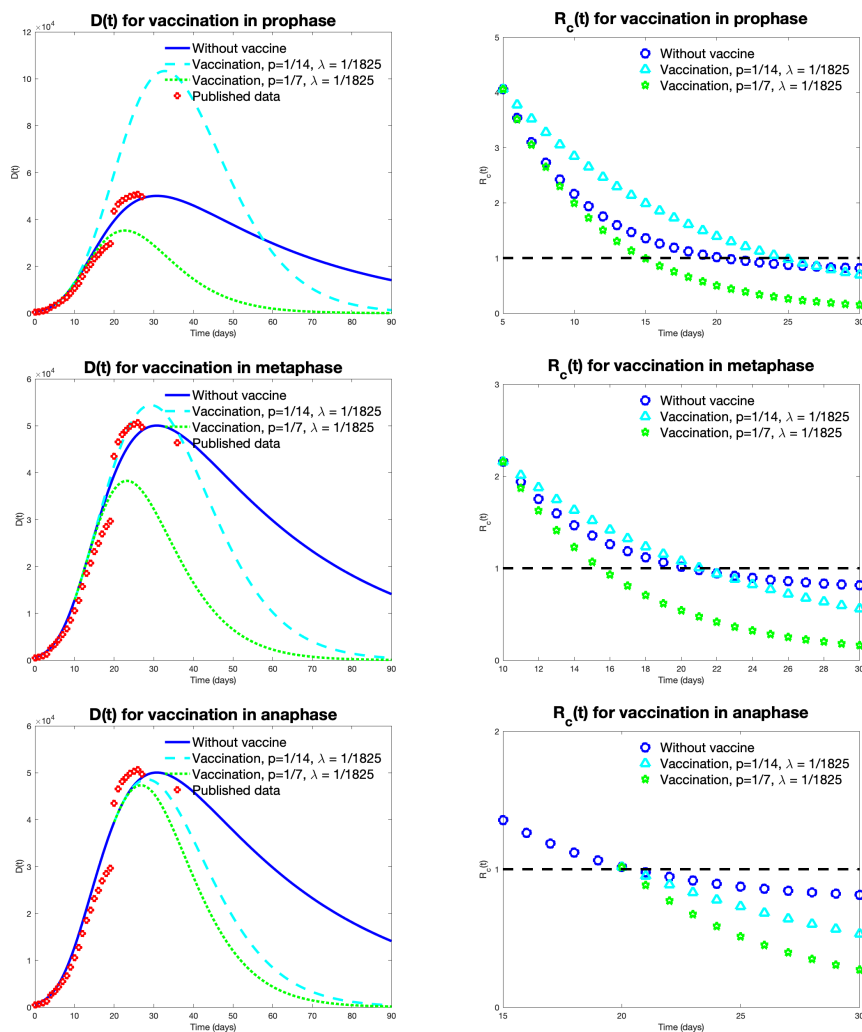


FIGURE 7. Impact of vaccination strategy inside Hubei Province

Province, we take the parameter p as $1/3$ and $1/7$ to compare with current control strategy ($p = 1/3$). We find that the application of vaccine accelerates the epidemic control process, bring the peak forward and reduce total amount of diagnostic population. The trends of $\mathcal{R}_c(t)$ with vaccine are much lower than those in current strategy. In the simulation inside Hubei, we take p as $1/7$ and $1/14$, which is smaller than the optimal simulation ($p = 1/6.2$). Broadly speaking, the effect will be greater as the parameter p increases. The vaccination strategy does an excellent job on reducing $\mathcal{R}_c(t)$ and effective action of taking the vaccine immunity is very important to prevent the growth of diagnostic population. Both inside and outside Hubei, the control of disease in prophase should be paid more attention. If the parameter p is smaller than that in isolation strategy, the peak value of $D(t)$ will be greater than current situation. It means that, in the prophase of control, it is

suitable for taking both vaccination and isolation strategy into account. Compared with isolation strategy, vaccination strategy is more convenient for our daily life and the effect can be long lasting.

4. CONCLUSION

The unprecedented isolation strategy in China has achieved great success in current control stage. Although the control reproduction number \mathcal{R}_c^0 is high, the effective control reproduction number $\mathcal{R}_c(t)$ decreases sharply under intervention. $\mathcal{R}_c(t)$ of outside Hubei down to the critical value on February 2, 2020, and in our simulation the value will maintain about 0.6 (see Figure 6b). In Hubei Province, $\mathcal{R}_c(t)$ reaches 1 on February 13, 2020, we can see that it is in a continued momentum of decline (see Figure 7b). To have a better understanding of the isolation strategy, we simulate, for each selected province, the goodness of fit which shows that the proposed model is suitable to describe the situation of control in China. We find that if the isolation period is not long enough, the strategy won't work. In Hubei Province, the quarantine period is simulated as 90 days and our results coincide with the study of Zhong's group [36]. In particular, our study suggests that the control period in Hubei is from January to the end of April. In the area outside Hubei, the trends of COVID-19 in most provinces between 30 days and 60 days isolation period are similar. Under careful personal protection, people can return to their normal daily life in these provinces.

After the outbreak of COVID-19, the China central government pushed a series of policies to ensure the medical care for patients, such as early diagnosis, early isolation, free treatment and etc. We discuss the peak value and peak time of $D(t)$ in many cases. An index called *AMR* is defined to measure the needs of medical resources. Sufficient medical resources are the basis of the control of the disease. So it is necessary to assign medical resources to deal with the shocks caused by booming demand of patients. To study the detail situation of each province, *AMR* and original medical power are both considered. We find that, the set up of designated hospital decreases the medical burden sharply. It releases the pressure of diagnosis and isolation in each provinces. But the situation of Hubei is still a crisis and the disease burden is still huge. Medical workers and materials are transferred to Hubei from other provinces to ensure the control of COVID-19.

There are many similarities between SARS and COVID-19, following this characteristic, we explored the relationship between the spread of COVID-19 and meteorological factors, which is considered as a key factor for the disappear of SARS. The impact of meteorological factors is different in high and low migration groups (see Table 6). Our results show that, air index is the most important meteorology factor. It is strongly suggests that for low *MiI* group, if the air condition is bad with strong wind, please pay more attention to the personal protection. High relative humidity is a positive factor for the COVID-19 control.

In the last part, we conducted some preparatory study on the coming new vaccine. The situations after the vaccine is brought into use are shown. We test the different starting times in each control phase inside and outside Hubei. Vaccination strategy is more convenient for daily control. But the development cycle of new vaccine is relatively long, the isolation strategy is still necessary in early control. The analysis helps design the final vaccination strategy once the new vaccine can be used by the general public. All of our study matches the actual control strategy

in China and the results are discussed adequately. Our study has the potential of providing a guideline for the control of COVID-19 in other countries.

APPENDIX

TABLE 7. Estimation of peak value, peak time of $D(t)$ and medical resource needed in 90 days.

$1/\lambda$	$Peak$	T_{peak}	AMR	$Peak$	T_{peak}	AMR	$Peak$	T_{peak}	AMR	$Peak$	T_{peak}	AMR
	Anhui			Beijing			Chongqing			Fujian		
data	777	20	-	295	21	-	423	20	-	228	19	-
60	770	20	28759k	275	19	10216k	398	18	12705k	227	19	8866k
30	905	25	46939k	322	24	16313k	436	20	18344k	344	37	25911k
20	1235	44	93412k	433	39	32269k	495	25	29820k	4989	*	135973k
10	66800	*	1231648k	27116	*	489384k	6186	*	181709k	1736757	*	18675280k
5	4348428	*	48700375k	2067882	*	24241821k	215309	*	2846363k	7237440	74	212118841k
	Gansu			Guangdong			Guangxi			Guizhou		
data	66	17	-	1007	18	-	193	23	-	117	20	-
60	59	15	1639k	988	18	32278k	191	21	8093k	109	21	4203k
30	63	16	2289k	1192	22	55932k	214	24	10768k	135	27	8058k
20	69	19	3609k	1692	40	128580k	249	30	15598k	343	*	19080k
10	718	*	23135k	257422	*	3953350k	2062	*	70888k	18929	*	299589k
5	37961	*	487756k	16571603	*	285227509k	97897	*	1273544k	1058173	*	10532875k
	Hainan			Hebei			Heilongjiang			Henan		
data	126	21	-	211	22	-	370	22	-	901	21	-
60	112	20	4078k	200	20	7495k	362	24	16787k	865	18	30486k
30	138	26	8172k	257	28	15477k	1120	*	62745k	1064	23	53455k
20	427	*	21573k	917	*	43993k	18180	*	382084k	1678	60	127687k
10	32644	*	471386k	102473	*	1343808k	3041233	*	35868972k	334575	*	4768513k
5	771931	*	11927662k	7477953	*	77594648k	7732929k	74	232380351k	17625745	*	334589749k
	Hunan			Inner Mongolia			Jiangsu			Jiangxi		
data	698	19	-	66	27	-	456	22	-	712	22	-
60	702	16	21867k	64	28	3167k	445	22	20035k	718	19	24493k
30	797	19	33027k	160	*	9703k	465	23	22492k	866	24	42908k
20	957	25	58685k	1882	*	43991k	487	25	25453k	1251	51	95956k
10	28641	*	670425k	300866	*	2807802k	579	32	37983k	112385	*	1870821k
5	3334809	*	39348405k	6566392	*	98519328k	1479	*	82541k	4696779	*	69937216k
	Jilin			Liaoning			Ningxia			Shaanxi		
data	73	17	-	97	17	-	43	22	-	189	20	-
60	62	19	2086k	95	18	3336k	42	18	1384k	187	18	6093k
30	69	21	2909k	126	26	8210k	46	21	1934k	203	19	8089k
20	79	26	4488k	892	*	32358k	51	25	2960k	223	22	11401k
10	780	*	25419k	255742	*	2739032k	385	*	13577k	816	*	40286k
5	46330	*	575506k	5402772	84	119906271k	8998	*	136715k	22248	*	391375k
	Shandong			Shanghai			Shanxi			Sichuan		
data	416	20	-	255	21	-	189	20	-	357	21	-
60	415	20	16992k	232	16	7036k	187	18	6093k	346	22	16921k
30	507	26	26645k	268	19	11108k	203	19	8089k	403	26	22616k
20	720	41	51630k	337	27	22023k	223	22	11401k	504	35	33486k
10	54739	*	955181k	25816	*	473809k	816	*	40286k	7264	*	207899k
5	11784044	*	116251444k	2900252	*	42717157k	22248	*	391375k	1016284	*	10516655k
	Tianjin			Xinjiang			Yunnan			Zhejiang		
data	99	21	-	63	23	-	135	22	-	921	16	-
60	82	22	3660k	58	25	2868k	131	18	5330k	905	17	28601k
30	90	25	4662k	77	35	5010k	139	20	6007k	1089	21	51192k
20	103	30	6341k	196	*	10834k	147	21	6861k	1642	*	127746k
10	526	*	21782k	10969	*	168818k	185	29	11161k	374851	*	5368778k
5	15458	*	236496k	1041128	*	8958716k	862	*	39412k	8395172	83	210982965k

¹ * do not reach peak in 90 days.

² - not applicable.

TABLE 8. Simulation parameter Part I

Parameter	Anhui	Beijing	Chongqing	Fujian	Gansu	Guangdong	Guangxi
β	2.7096E-08	9.1997E-08	3.6320E-08	9.6503E-08	6.2034E-08	2.7096E-08	2.7083E-08
θ	0.1100	0.0110	0.0800	0.0900	0.0100	0.0050	0.0050
p	1/4.1	1/4	1/6.4	1/3	1/6.5	1/3	1/4
λ	1/60	1/60	1/60	1/60	1/60	1/60	1/60
σ	1/7	1/7	1/7	1/7	1/7	1/7	1/7
ρ	0.9000	0.9400	0.9900	0.9300	0.9000	0.9100	0.8800
ϵ_A	1/7	1/8	1/9	1/5	1/7	1/10	1/10
ϵ_I	1/5	1/4	1/4.5	1/4	1/4	1/3.3	1/4.5
γ_A	0.0993	0.0996	0.1190	0.0988	0.2597	0.1075	0.0579
γ_I	0.0736	0.0766	0.0992	0.0882	0.1998	0.0716	0.0386
γ_D	0.0883	0.0843	0.1487	0.0970	0.2398	0.1039	0.0560
d_I	0.0027	0.0026	0.0040	0.0022	0.0073	0.0024	0.0013
d_D	0.0018	0.0017	0.0033	0.0015	0.0049	0.0016	0.0009
R_c	5.0939	5.1544	3.0885	6.4914	2.9989	6.3126	3.7215
S(0)	56912400	19601400	27918000	24434200	24524100	96441000	40885800
Q(0)	6323600	1938600	3102000	14975800	1845900	17019000	8374200
E(0)	591	123	580	80	175	886	95
A(0)	288	81	90	65	50	37	52
I(0)	101	58	88	50	5	93	49
D(0)	15	26	27	10	2	51	13
R(0)	6	0	0	0	0	2	0
	Guizhou	Hainan	Hebei	Heilongjiang	Henan	Hunan	Inner Mongolia
β	4.9543E-08	1.8064E-07	2.7096E-08	7.9315E-08	3.5675E-08	2.9823E-08	8.8785E-08
θ	0.0500	0.1000	0.0300	0.2000	0.2000	0.1000	0.0130
p	1/4.5	1/5	1/5	1/3.5	1/3	1/3	1/5
λ	1/60	1/60	1/60	1/60	1/60	1/60	1/60
σ	1/7	1/7	1/7	1/7	1/7	1/7	1/7
ρ	0.7000	0.9000	0.9000	0.9500	0.8900	0.9100	0.9700
ϵ_A	1/15	1/10	1/7	1/7	1/4	1/10	1/5
ϵ_I	1/9	1/6	1/4	1/5	1/3	1/5.1	1/4
γ_A	0.1298	0.1495	0.1085	0.0967	0.0993	0.1085	0.0709
γ_I	0.0998	0.0997	0.0724	0.0744	0.0764	0.0986	0.0473
γ_D	0.1098	0.1396	0.1049	0.0818	0.0840	0.1085	0.0662
d_I	0.0008	0.0045	0.0024	0.0026	0.0026	0.0035	0.0020
d_D	0.0006	0.0030	0.0021	0.0018	0.0017	0.0023	0.0014
R_c	3.9208	5.1065	3.8753	6.2331	6.6235	3.5025	6.5656
S(0)	23400000	8406000	51380800	22638000	83563500	37944500	22806000
Q(0)	12600000	934000	24179200	15092000	12486500	31045500	2534000
E(0)	280	110	168	308	556	1500	16
A(0)	28	45	40	25	211	145	9
I(0)	8	25	33	15	22	65	4
D(0)	3	8	1	3	9	24	2
R(0)	0	0	0	0	0	0	0

TABLE 9. Simulation parameter Part II

Parameter	Jiangsu	Jiangxi	Jilin	Liaoning	Ningxia	Shaanxi	Shandong
β	5.0000E-09	4.8409E-08	4.7838E-08	6.9683E-08	1.5932E-07	2.8218E-08	2.7094E-08
θ	0.2000	0.2000	0.0050	0.0100	0.1000	0.0900	0.2000
p	1/5	1/4.5	1/4	1/3	1/7.9	1/4.5	1/3
λ	1/60	1/60	1/60	1/60	1/60	1/60	1/60
σ	1/7	1/7	1/7	1/7	1/7	1/7	1/7
ρ	0.9800	0.8000	0.9600	0.9500	0.9000	0.7000	0.9800
ϵ_A	1/10	1/10	1/6	1/10	1/5	1/10	1/5
ϵ_I	1/7	1/3.9	1/5	1/5	1/4	1/9	1/3
γ_A	0.0474	0.1296	0.1029	0.1196	0.1462	0.1298	0.0618
γ_I	0.0379	0.0997	0.0686	0.0997	0.0975	0.0999	0.0515
γ_D	0.0455	0.1087	0.0960	0.1296	0.1365	0.1098	0.0567
d_I	0.0010	0.0037	0.0029	0.0007	0.0042	0.0009	0.0017
d_D	0.0007	0.0023	0.0020	0.0007	0.0028	0.0006	0.0012
R_c	1.8970	4.3156	4.2087	6.7287	2.4398	2.2381	6.2478
S(0)	70041090	37184000	24877352	30513000	5916800	23184000	90423000
Q(0)	10465910	9296000	2163248	13077000	963200	15456000	10047000
E(0)	452	840	87	44	70	640	165
A(0)	145	50	6	25	5	36	60
I(0)	125	67	5	38	4	20	36
D(0)	9	7	3	4	3	5	15
R(0)	0	0	0	0	0	0	0
	Shanghai	Shanxi	Sichuan	Tianjin	Xinjiang	Yunnan	Zhejiang
β	1.2638E-07	8.1979E-08	2.7018E-08	1.4151E-07	7.0499E-08	2.2519E-08	5.7383E-08
θ	0.0100	0.1000	0.1100	0.0050	0.0100	0.0900	0.1000
p	1/3	1/3	1/3	1/5	1/4	1/3.2	1/3
λ	1/60	1/60	1/60	1/60	1/60	1/60	1/60
σ	1/7	1/7	1/7	1/7	1/7	1/7	1/7
ρ	0.9200	0.9000	0.9200	0.9000	0.8900	0.9800	0.9600
ϵ_A	1/4	1/3	1/4	1/10	1/9	1/4	1/6
ϵ_I	1/3	1/2.5	1/3	1/4	1/5	1/3	1/3
γ_A	0.1213	0.0809	0.0387	0.1254	0.0540	0.0491	0.1190
γ_I	0.0808	0.0622	0.0322	0.0836	0.0415	0.0327	0.0793
γ_D	0.1132	0.0685	0.0355	0.1170	0.0457	0.0458	0.1150
d_I	0.0035	0.0001	0.0011	0.0036	0.0014	0.0014	0.0017
d_D	0.0023	0.0001	0.0007	0.0024	0.0009	0.0009	0.0012
R_c	5.6066	5.4060	5.1509	5.2949	4.2468	2.6164	6.9822
S(0)	20119200	33462000	75069000	14036400	16412616	43465500	52206700
Q(0)	4120800	3718000	8341000	1559600	8454984	4829500	5163300
E(0)	266	48	140	40	40	134	456
A(0)	22	21	64	26	11	12	145
I(0)	11	8	28	15	5	10	133
D(0)	19	1	15	8	2	5	42
R(0)	3	0	0	0	0	0	1

Acknowledgments. This work was partially supported by National Natural Science Foundation of China (Grant No. 41704116, 11901234, 11926104), Jilin Provincial Excellent Youth Talents Foundation (Grant No. 20180520093JH), Scientific Research Project of Education Department of Jilin Province (Grant No. JJKH20200933KJ).

REFERENCES

- [1] Baidu Map Website. <http://map.baidu.com/>
- [2] Baidu Migration Website. <http://qianxi.baidu.com/>
- [3] Bogoch, I.; Watts, A.; Thomas-Bachli, A.; et al.; *Pneumonia of unknown aetiology in Wuhan, China: potential for international spread via commercial air travel*, Journal of Travel Medicine, 1 (2020).
- [4] Chan, J.; Yuan, S.; Kok, K.; et al.; *A familial cluster of pneumonia associated with the 2019 novel coronavirus indicating person-to-person transmission: a study of a family cluster*, The Lancet, 395(10223) (2020), 514-523.
- [5] Chen, T.; Rui, J.; Wang, Q.; et al.; *A mathematical model for simulating the transmission of Wuhan novel Coronavirus*, bioRxiv:2020.01.19.911669, (2020).
- [6] Chen, Y.; Cheng, J.; Jiang, Y.; et al.; *A Time Delay Dynamical Model for Outbreak of 2019-nCoV and the Parameter Identification*, arXiv:2002.00418, (2020).
- [7] Chen, Z.; Ye, D.; Yang, H.; et al.; *A comparative study on the relationship between the epidemic of atypical pneumonia, meteorology and climate in various parts of China*, (in Chinese). Hubei Province Science and Technology Association. (2004), 23-28.
- [8] Chen, Z.; Ye, D.; Yang, H.; et al.; *Relationship between SARS and meteorological factors in various parts of China*, (in Chinese). Meteorology, 2 (2004), 42-45.
- [9] China Meteorological Data Service Center Website. <http://data.cma.cn/>
- [10] Coronavirus: Common Symptoms, Preventive Measures, & How to Diagnose It; <https://www.caringlyyours.com/coronavirus/>, Caringly Yours. Retrieved January 28, 2020.
- [11] COVID-19 Information Release Platform of Zhejiang Province; <http://www.blueskyinfo.com.cn/wjwApp/webinfo/infoList.do>, Retrieved February 24, 2020.
- [12] Diagnosis and treatment of novel coronavirus pneumonia. (trial version Sixth, in Chinese.)
- [13] Driessche, P.; Watmough, J.; *Reproduction numbers and sub-threshold endemic equilibria for compartmental models of disease transmission*, Mathematical Biosciences. 180(1) (2002), 29-48.
- [14] Guan, W.; Ni, Z.; Hu, Y.; et al.; *Clinical characteristics of 2019 novel coronavirus infection in China*, medRxiv:2020.02.06.20020974, (2020).
- [15] Li, Q.; Guan, X.; Wu, P.; et al.; *Early Transmission Dynamics in Wuhan, China, of Novel Coronavirus-Infected Pneumonia*, New England Journal of Medicine, (2020).
- [16] Liu, S.; Li Y.; Bi, Y.; et al.; *Mixed vaccination strategy for the control of tuberculosis: A case study in China*, Mathematical Biosciences and Engineering, 14(3) (2017), 695-708.
- [17] Ming, W.; Huang, J.; Zhang, C.; *Breaking down of healthcare system: Mathematical modelling for controlling the novel coronavirus (2019-nCoV) outbreak in Wuhan, China*, bioRxiv:2020.01.27.922443, (2020).
- [18] Miriam, D.; Kanta, S.; Stephen, M.; et al.; *Inactivation of the coronavirus that induces severe acute respiratory syndrome, SARS-CoV*, Journal of Virological Methods, 121(1) (2004), 85-91.
- [19] Mutua, J. M.; Barker, C. Y.; Vaidya, N. K.; *Modeling impacts of socioeconomic status and vaccination programs on typhoid fever epidemics*, Electronic Journal of Differential Equations, Conference 24 (2017), 63-74.
- [20] National Bureau of Statistics Website. <http://www.stats.gov.cn/>
- [21] Pang, L.; Ruan, S.; Liu, S.; et al.; *Transmission dynamics and optimal control of measles epidemics*, Applied Mathematics And Computation, 256 (2015), 131-147.
- [22] Phan, L.; Nguyen, T.; Luong, Q.; et al.; *Importation and Human-to-Human Transmission of a Novel Coronavirus in Vietnam*, New England Journal of Medicine, 382(9) (2020), 872-874.
- [23] Pradeep, B. G. S. A.; Ma, W.; *Global stability of a delayed mosquito-transmitted disease model with stage structure*, Electronic Journal of Differential Equations, 2015(10) (2015), 1-19.

- [24] Report of the WHO-China joint mission on Coronavirus disease 2019 (COVID-19).
- [25] Rothe, C.; Schunk, M.; Sothmann, P.; et al.; *Transmission of 2019-nCoV Infection from an Asymptomatic Contact in Germany*, New England Journal of Medicine, 382(10) (2020), 970-971.
- [26] Shen, M.; Xiao, Y.; Rong, L.; *Modeling the effect of comprehensive interventions on Ebola virus transmission*, Scientific Reports, 5(15818) (2015).
- [27] Tang, B.; Wang, X.; Li, Q.; et al.; *Estimation of the Transmission Risk of the 2019-nCoV and Its Implication for Public Health Interventions*, Journal of Clinical Medicine, 9(2) (2020), 462.
- [28] Tang, B.; Zhou, W.; Xiao, Y.; et al.; *Implication of sexual transmission of Zika on dengue and Zika outbreaks*, Mathematical Biosciences and Engineering, 16(5) (2019), 5092-5113.
- [29] WHO Director-General's opening remarks at the media briefing on COVID-19. <https://www.who.int/en/dg/speeches/>. Retrieved February 28, 2020.
- [30] Wikipedia Website; <https://en.wikipedia.org/wiki/Coronavirus/>.
- [31] World Health Organization Website. <https://www.who.int/>
- [32] Wrapp, D.; Wang, N.; Corbett, K.; et al.; *Cryo-EM structure of the 2019-nCoV spike in the prefusion conformation*, Science, 2 (2020), eabb2507.
- [33] Wu, J.; Leung, K.; Leung, G.; *Nowcasting and forecasting the potential domestic and international spread of the 2019-nCoV outbreak originating in Wuhan, China: a modelling study*, The Lancet, 395(10225) (2020), 689-697.
- [34] Xia, Z.; Zhang, J.; Xue, Y.; et al.; *Modeling the Transmission of Middle East Respirator Syndrome Corona Virus in the Republic of Korea*, PLoS ONE, 10(12) (2015), e0144778.
- [35] Yang, Y.; Lu, Q.; Liu, M.; et al.; *Epidemiological and clinical features of the 2019 novel coronavirus outbreak in China*, medRxiv:2020.02.10.20021675, (2020).
- [36] Yang, Z.; Zeng, Z.; Wang, K.; et al.; *Modified SEIR and AI prediction of the epidemics trend of COVID-19 in China under public health interventions*, Journal of Thoracic Disease, 12(2) (2020).
- [37] Zhou, Y.; Ma, Z.; Brauer, F.; *A discrete epidemic model for SARS transmission and control in China*, Mathematical and Computer Modelling, 40(13) (2004), 1491-1506.
- [38] Zou, L.; Zhang, W.; Ruan S.; *Modeling the transmission dynamics and control of hepatitis B virus in China*, Journal of Theoretical Biology, 262(2) (2010), 330-338.
- [39] Zhu, N.; Zhang, D.; Wang, W.; et al.; *A Novel Coronavirus from Patients with Pneumonia in China, 2019*, New England Journal of Medicine, 382 (2020), 727-733.

JIWEI JIA

SCHOOL OF MATHEMATICS, JILIN UNIVERSITY, CHANGCHUN, JILIN 130012, CHINA.
INTERDISCIPLINARY CENTER OF JILIN PROVINCE FOR APPLIED MATHEMATICS, CHANGCHUN, JILIN 130012, CHINA

Email address: jjajjwei@jlu.edu.cn

JIAN DING

SCHOOL OF MATHEMATICS, JILIN UNIVERSITY, CHANGCHUN, JILIN 130012, CHINA

Email address: dingjian17@mails.jlu.edu.cn

SIYU LIU (CORRESPONDING AUTHOR)

SCHOOL OF PUBLIC HEALTH, JILIN UNIVERSITY, CHANGCHUN, JILIN 130021, CHINA

Email address: liusiyu@jlu.edu.cn

GUIDONG LIAO

SCHOOL OF MATHEMATICS, JILIN UNIVERSITY, CHANGCHUN, JILIN 130012, CHINA

Email address: liaogd18@mails.jlu.edu.cn

JINGZHI LI

DEPARTMENT OF MATHEMATICS, SOUTHERN UNIVERSITY OF SCIENCE AND TECHNOLOGY, SHENZHEN, GUANGDONG 518055, CHINA

Email address: lijz@sustech.edu.cn

BEN DUAN

SCHOOL OF MATHEMATICAL SCIENCES, DALIAN UNIVERSITY OF TECHNOLOGY, DALIAN, LIAONING
116024, CHINA

Email address: bduan@dlut.edu.cn

GUOQING WANG

SCHOOL OF BASIC MEDICAL SCIENCE, JILIN UNIVERSITY, CHANGCHUN, JILIN 130021, CHINA

Email address: qing@jlu.edu.cn

RAN ZHANG

SCHOOL OF MATHEMATICS, JILIN UNIVERSITY, CHANGCHUN, JILIN 130012, CHINA.

INTERDISCIPLINARY CENTER OF JILIN PROVINCE FOR APPLIED MATHEMATICS, CHANGCHUN, JILIN
130012, CHINA

Email address: zhangran@jlu.edu.cn